time. As is evident from the Figures and Table 3, the two carboxyl groups do not have identical surroundings; possible implications of the situation in relation to the asymmetry of the tartrate ion have been discussed in the previous paragraph.

The neutron diffraction data confirm the hydrogen-bonding scheme deduced from the X-ray data. As has been noted in previously determined compounds, the values of the O–H and C–H bond distances (Table 4) from neutron data are about 0·15 Å longer than those determined from X-ray data (Fig. 3). This discrepancy is due to an inadequate description of the X-ray scattering from a bound hydrogen atom (for form factors of bonded hydrogen atoms, see Stewart, Davidson & Simpson, 1965). The bond distances derived from the neutron diffraction data are closer to accepted values. In addition, the two O–H–O hydrogen bond angles (Table 3) which were found to be less than 160° by X-rays are shown to be closer to 170°. We note that the expected inverse relationship between O–H and O–O distance in hydrogen bonds seems to hold in this compound, although the accuracy of the determination is not really high enough to be certain about it.

We would like to thank Dr W.C. Hamilton, of the Brookhaven National Laboratory, for performing the least-squares calculations with the neutron diffraction data.

References

BOMMEL VAN, A. J. & BIJVOET, J. M. (1958). *Acta Cryst.* **11**, 1961.
COLE, H., OKAYA, Y. & CHAMBERS, F. W. (1963). *Rev. Sci. Instrum.* **34**, 872.
DONOHUE, J. (1952). *J. Chem. Phys.* **56**, 502.
International Tables for X-ray Crystallography (1962). Birmingham: Kynoch Press.
KROON, J., PEERDEMAN, A. F. & BIJVOET, J. M. (1965). *Acta Cryst.* **19**, 293.
KUMRA, S. K. & DARLOW, S. F. (1965). *Acta Cryst.* **18**, 98.
OKAYA, Y. (1964). *Control Programs for Computer-Controlled Diffractometers.* IBM Internal Report.
OKAYA, Y. (1965). *Acta Cryst.* **19**, 879.
OKAYA, Y. (1966). ACA Meeting, Austin, Texas. B-5.
STERN, F. & BEEVERS, C. A. (1950). *Acta Cryst.* **3**, 341.
STEWART, R. F., DAVIDSON, E. R. & SIMPSON, W. T. (1965). ACA 1965 Spring Meeting, A-5, Suffern, N.Y.

Acta Cryst. (1966). **21**, 243

X-ray Diffraction Study of Cold-worked α-CuIn and α-CuSn Alloys

BY K.N. GOSWAMI, S.P. SEN GUPTA AND M.A. QUADER
Indian Association for the Cultivation of Science, Calcutta 32, *India*

(*Received* 29 *December* 1965)

X-ray diffraction line profiles from filings of copper-indium and copper-tin alloys in the solid solution range were recorded by a Geiger counter X-ray diffractometer. Information regarding stacking fault densities α and β was obtained from peak-position and peak-asymmetry measurements and both parameters were found to increase with increasing solute concentration. The same general behaviour of the stacking-fault parameter α with respect to solute concentration was observed in the two systems and α increases in the order Cu–In, Cu–Sn. The broadening of the powder peaks was studied by Fourier analysis of line shapes, and the anisotropic values of the effective particle sizes $[D_e]_{hkl}$ and the root mean squared strains $[\langle \varepsilon_L^2 \rangle]_{hkl}^{1/2}$ were obtained in all cases. The measured effective particle sizes are primarily a consequence of deformation and twin faulting. A fair agreement was observed for the compound fault probability $(1{\cdot}5\alpha+\beta)$ obtained by two different methods.

1. Introduction

Cold working or plastic deformation of metals and alloys has been found to produce appreciable changes in the intensity distribution of diffracted X-rays. The changes in position, shape and width of X-ray powder diffraction line profiles from cold-worked metals and alloys are evidences of microstructural changes in the materials. The earlier X-ray studies in this field were usually confined to measurements of line-widths and it was suggested that line broadening is produced either by lattice strains or by lattice strains and small particle size simultaneously (Greenough, 1952). It was Barrett (1950), who first suggested that plastic deformation of face-centred cubic metals may introduce stacking faults on the (111) planes. Subsequently, Paterson (1952), Warren & Warekois (1955), and Wagner (1957*a*, *b*) developed the effects of deformation and twin stacking faults on the diffraction profiles of f.c.c. structures. If the normal stacking sequence of (111) planes is *ABCABC*, then a deformation fault is a break in this sequence *ABC'BCABC* where the prime indicates the fault plane. A reversal in the sequence *ABCACBA* represents a twin fault. Deformation faults give rise to a symmetrical broadening and peak-shift, while twin faults produce an asymmetrical broadening and a negligibly small peak-shift. In addition to the broadening due to faulting, the peaks of cold-worked

f.c.c. metals are broadened by a reduction in the size of the coherently diffracting domains as well as by the distortion within each domain. Information concerning the magnitudes of domain size, residual strains and the stacking fault density may be obtained satisfactorily by measuring the shape of a powder pattern line with sufficient accuracy and interpreting it in terms of Fourier coefficients (Warren 1959).

Extensive studies of the effect of alloying on the stacking fault probability have been made in copper base alloys (Warren & Warekois, 1955; Wagner, 1957; Smallman & Westmacott, 1957; Davies & Cahn, 1962; Foley, Cahn & Raynor, 1963; Vassamillet & Massalski, 1964) and all these investigations have shown the pronounced increase of fault probability with increasing solute concentration. Similar results have been also found for silver-base alloys (Adler & Wagner, 1962; Vassamillet & Massalski, 1963; Sen Gupta & Quader, 1966). Moreover, it was also observed that there exist possible correlations between the stacking-fault parameter α and the solute valency and electron-atom ratio in alloy systems based on a given solvent (Davies & Cahn, 1962).

The present investigation deals with the cold-worked copper–indium and copper–tin alloys in the solid solution range, and has been undertaken with a view to obtaining information concerning (i) the concentration of stacking faults in the alloys, (ii) the effect of polyvalent solutes on the occurrence of stacking faults, (iii) the nature of particle sizes and r.m.s. strains in the deformed condition and (iv) the role of different contributors in the observed line broadening effect.

2. Experimental procedure

The alloys used in this study were prepared from spectrographically standardized metals copper, indium and tin supplied by Johnson, Matthey and Co., Ltd, London. Accurately weighed quantities of the component metals, sufficient to give 8-g ingots, were melted together in evacuated and sealed quartz capsules; after melting, the alloys were homogenized for a week in the temperature range 600–800 °C. The annealing treatments were terminated by quenching in air. Weight changes during preparation were negligible. Different alloys of copper–indium and copper–tin with varying solute content were prepared in the solid solution range.

Cold working was achieved by hand filing at room temperature (25 ± 1 °C). A sample of the filings was retained in the 'as-filed' condition and another sample was annealed at 600 °C for 4 hours in a Pyrex glass capsule sealed under vacuum. After sieving through a 250 mesh screen, samples of the filings were bonded with a solution of Canada balsam in xylene and mounted in a recess in a specially designed aluminum holder which could itself be mounted in the specimen position of the diffractometer. The line profiles were recorded with the standard Philips Geiger Counter X-ray Diffractometer (PW 1050, 1051) with Ni-filtered Cu $K\alpha$ radiation from a highly stabilized X-ray generator (PW 1010). Accurate line profiles of the reflexions were obtained by point counting at intervals of 0·1° in 2θ for the general background, decreasing to 0·01° in 2θ near the maxima of the peaks, where 2θ is the Bragg angle. All the measurements were carried out at room temperature (25 ± 1 °C). No phase transformation due to cold working has been observed in the alloys with higher solute contents although at room temperature they are a mixture of two phases.

3. Experimental results

A. Peak position measurements

Peak position measurement leads to a direct determination of the deformation fault probability. Thus, the fault probability α is obtained from the change in separation of 111 and 200 reflexions using the relation (Wagner, 1957*a*):

$$(2\theta^\circ_{hkl}-2\theta^\circ_{h'k'l'})_{\mathrm{CW}}-(2\theta^\circ_{hkl}-2\theta^\circ_{h'k'l'})_{\mathrm{Ann}}=H\,.\,\alpha \quad (1)$$

and

$$H=(\langle G\rangle j\,.\,\tan\theta^\circ)_{hkl}-(\langle G\rangle j\,.\,\tan\theta^\circ)_{h'k'l'},$$

where j is the fraction of (hkl) planes affected by deformation faults, $G=(\pm)90\sqrt{3}\,.\,h_3/\pi^2 l_0^2$ and $\langle G\rangle$ is the averaged value for the hkl reflexions affected by deformation faults.

The peak positions of 111 and 200 reflexions were determined by the same method as adopted earlier (Sen Gupta & Quader, 1966), *i.e.* by taking the midpoints of section lines drawn parallel to the background level and extrapolating to the peak maximum. The estimated accuracy of the position measurements was about ±0·01° in 2θ. Elimination of the α_2 component in the case of cold-worked peaks was not possible since the graphical methods of Rachinger (1948) and of Papoulis (1955) could not be applied for broad, overlapping and asymmetric line profiles. Owing to statistical fluctuations, points of maximum intensity cannot be taken as a position for the peak maximum. Recently, Vassamillet & Massalski (1964) have critically analysed the difficulties encountered in peak position measurements.

Tables 1 and 2 show the values of α for Cu–In and Cu–Sn alloys respectively and the variation of α with electron concentration is shown in Fig. 1.

B. Peak asymmetry measurements

Twin faults have been found to broaden the diffraction line profiles asymmetrically. Cohen & Wagner (1962) have developed a method of determining twin fault probability β measuring the displacement of the centre of gravity of a peak from the peak maximum. By combining ΔCG ($^\circ 2\theta$), which is the displacement of the centre of gravity from the peak maximum, for 111 and 200 reflexions partial compensation for systematic and instrumental effects can be achieved.

The following relation is involved in the determination of β:

$$\beta = \frac{\Delta CG\,(^\circ 2\theta)_{111} - \Delta CG\,(^\circ 2\theta)_{200}}{11\tan\theta_{111} + 14{\cdot}6\tan\theta_{200}} \qquad (2)$$

The method of Ladell, Parrish & Taylor (1959) has been adopted for the determination of the centre of gravity of line profiles. Prior to actual evaluation of the centre of gravity, each peak height was divided by the factor (Warren, 1959) $f^2(1+\cos^2 2\theta)/\sin^2\theta$, where f is the atomic scattering factor. However, experimental limitations (such as long tails of the peak, peak overlap and the error in the peak maximum position determination) do not enable us to obtain an accurate determination of ΔCG and hence a good accuracy in the values of β.

Values of β are inserted in Tables 1 and 2. Fig. 2 shows the variation of the reciprocal stacking fault probabilities α^{-1} and β^{-1} as a function of solute concentration.

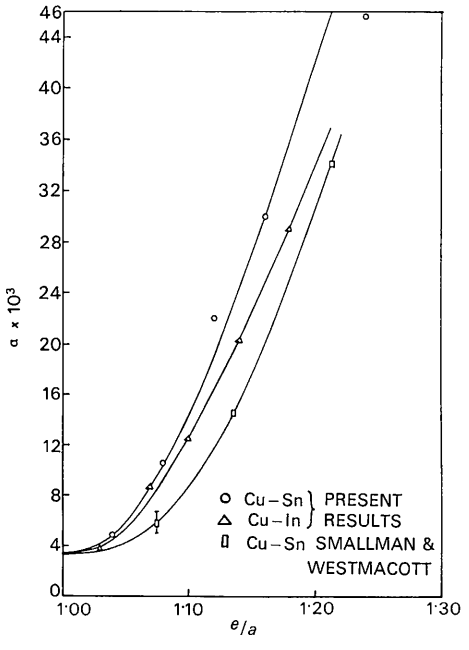

Fig. 1. Deformation fault probability α as a function of electron concentration e/a in copper-base alloys.

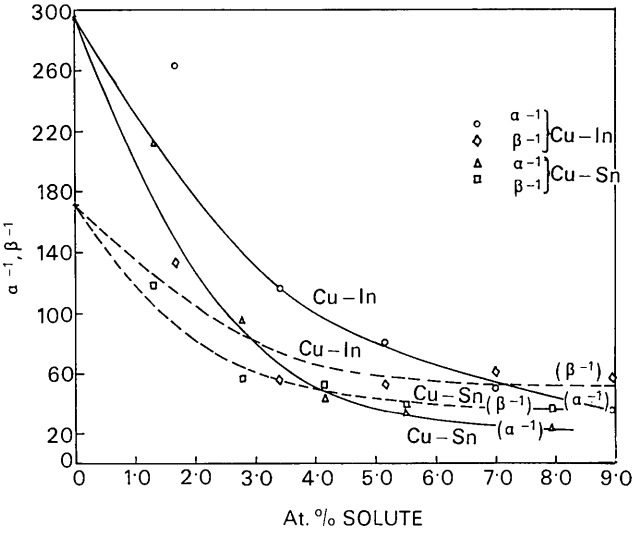

Fig. 2. Variation of reciprocal deformation fault probability α^{-1} and reciprocal twin fault probability β^{-1} as a function of indium and tin concentration.

C. Peak broadening measurements

Fourier analysis of line shapes provides information about the effective particle size, the r.m.s. strain distribution and the compound faulting probability $(1{\cdot}5\alpha+\beta)$. Warren & Averbach's method (Warren, 1959) has been adopted in order to separate the effect of particle size and strain on the peak broadening and the 111, 222, 200 and 400 reflexions were chosen. Initially, Stokes's method (1948) has been applied for the correction of instrumental broadening. It has been assumed that line shapes obtained from the samples annealed for 4 hours at 600 °C are, in each case, an exact measure of instrumental broadening. Fourier coefficients expressing the line shapes were obtained by means of Beevers–Lipson strips, and the corrected coefficients were represented as A_L *versus* L where L $(=na_3)$ has the significance of a distance normal to the reflecting planes. The curves are in the order 111, 222, 200 and 400 rather than in the order of $(h^2+k^2+l^2)$.

The measured coefficients A_L may be written:

$$\ln A_L(h_0) = \ln A_L^P + \ln A_L^D(h_0)\,, \qquad (3)$$

where A_L^P are the particle size coefficients and A_L^D are the strain coefficients dependent upon $h_0=(h^2+k^2+l^2)^{\frac{1}{2}}$, the order of reflexion.

For a Gaussian strain distribution,

$$A_L^D = \exp\left(-2\pi^2 L^2\langle\varepsilon_L^2\rangle h_0^2/a^2\right), \qquad (4)$$

where a is the lattice parameter and ε_L is the mean strain between any two points a distance L apart normal to the reflecting planes. $\langle\varepsilon_L^2\rangle$ is the mean strain, squared and averaged over the specimen.

The Fourier coefficients were interpreted by plotting $\ln A_L$ against h_0^2 for various values of L. Logarithmic plots were done for two sets of multiple orders (111)–(222) and (200)–(400). The intercepts of these curves at $h_0^2=0$ give Fourier coefficient A_L^P and the slopes give $\langle\varepsilon_L^2\rangle$ from which r.m.s. strains are obtained for [111] and [100] directions. Plots of A_L^P obtained from *hkl* reflexions are then made as a function of L and the intercepts on L of the initial slope give the effective particle size $[D_e]_{hkl}$. 'Hook effect' (Warren, 1959) was not observed in the region of small L. Tables 1 and 2 summarize the values of $[D_e]_{hkl}$ and $[\langle\varepsilon_{L=50\text{ Å}}^2\rangle]_{hkl}^{\frac{1}{2}}$ for Cu–In and Cu–Sn alloys respectively. Figs. 3 and 4 show the plots of A_L^P and $\langle\varepsilon_L^2\rangle^{\frac{1}{2}}$ as a function of distance L for both [111] and [100] directions in the Cu – 8·94 In alloy. Fig. 5 illus-

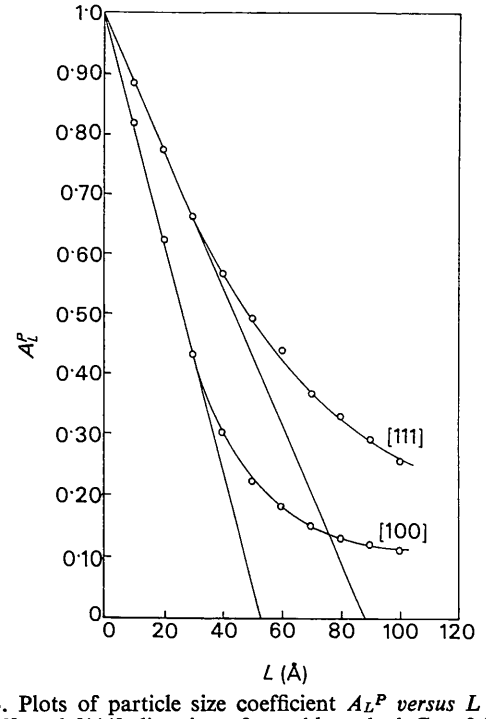

Fig. 3. Plots of particle size coefficient A_L^P *versus* L for the [100] and [111] directions for cold-worked Cu–8·94% In alloy. The intercepts on L of the initial slope give effective particle size $[D_e]_{hkl}$.

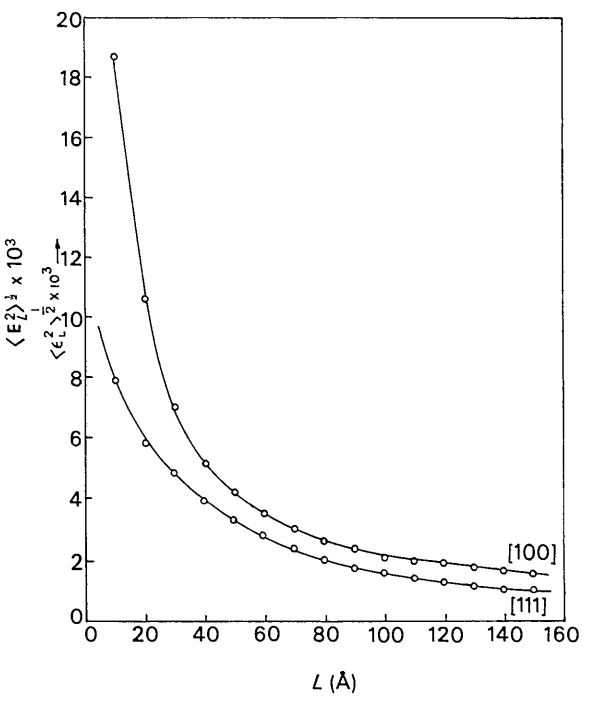

Fig. 4. Variation of r.m.s. strain $\langle \epsilon_L^2 \rangle^{\frac{1}{2}}$ as a function of averaging distance L for [100] and [111] directions for cold-worked Cu–8·94% In alloy.

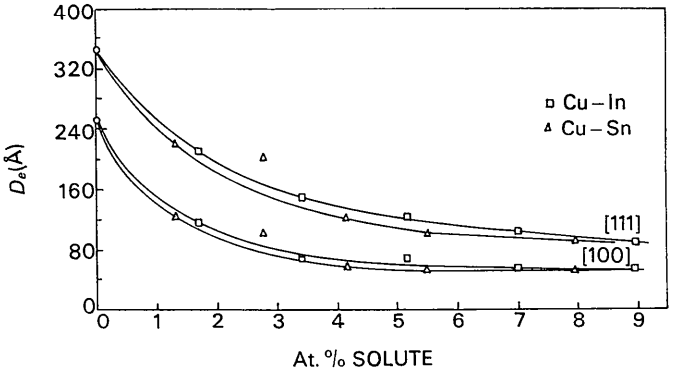

Fig. 5. Variation of the effective particle size in the [*hkl*] directions $[D_e]_{hkl}$ as a function of indium and tin concentration.

Table 1. *Experimental results for copper-indium alloys*

Composition (at. %)	$\alpha \times 10^3$	$\beta \times 10^3$	$(1{\cdot}5\alpha+\beta)_{M+A} \times 10^3$	$(1{\cdot}5\alpha+\beta)_B \times 10^3$	$[D_{SF}]_{111}$ (Å)	$[D_e]_{111}$ (Å)	$[D_e]_{100}$ (Å)	T_{min} (Å)	$[\langle \varepsilon^2_{L=50\,Å} \rangle]_{111}^{\frac{1}{2}} \times 10^3$	$[\langle \varepsilon^2_{L=50\,Å} \rangle]_{100}^{\frac{1}{2}} \times 10^3$
Cu	3·40	5·86	11	7	761	344	252	299	2·01	2·06
Cu–1·67 In	3·80	7·50	13	26	636	215	116	400	3·05	4·25
Cu–3·41 In	8·60	17·96	31	46	273	138	69	364	2·89	4·15
Cu–5·16 In	12·48	19·15	38	42	223	122	68	194	2·86	4·17
Cu–6·99 In	20·28	16·71	47	52	180	93	53	137	3·45	4·16
Cu–8·94 In	29·14	17·82	61	50	139	87	52	112	3·28	4·19

Table 2. *Experimental results for copper-tin alloys*

Composition (at. %)	$\alpha \times 10^3$	$\beta \times 10^3$	$(1{\cdot}5\alpha+\beta)_{M+A} \times 10^3$	$(1{\cdot}5\alpha+\beta)_B \times 10^3$	$[D_{SF}]_{111}$ (Å)	$[D_e]_{111}$ (Å)	$[D_e]_{100}$ (Å)	T_{min} (Å)	$[\langle \varepsilon^2_{L=50\,Å} \rangle]_{111}^{\frac{1}{2}} \times 10^3$	$[\langle \varepsilon^2_{L=50\,Å} \rangle]_{100}^{\frac{1}{2}} \times 10^3$
Cu	3·40	5·86	11	7	761	344	252	299	2·01	2·06
Cu–1·31 Sn	4·75	8·48	16	22	537	220	125	328	2·88	4·02
Cu–2·77 Sn	10·48	17·84	33	31	251	201	102	485	3·53	4·56
Cu–4·14 Sn	23·00	19·13	54	58	158	121	58	443	3·46	4·87
Cu–5·51 Sn	29·86	26·01	71	58	120	101	53	205	3·84	4·71
Cu–7·95 Sn	45·59	28·83	97	55	88	90	51	135	4·01	4·76

trates the decrease in effective particle size as the indium and tin concentration increases in the copper alloys.

4. Discussion

Values of the stacking fault parameter α for the copper–indium and copper–tin alloys investigated are given in Tables 1 and 2 respectively and plotted as functions of electron/atom ratio in Fig. 1, which also shows the previous results of Smallman & Westmacott (1957) for the copper–tin alloys. It is seen from the Fig. 1 that for both copper–indium and copper–tin alloys the stacking fault parameter α increases slowly up to about 1·10 electrons per atom and beyond this electron/atom ratio the curves rise steeply as the solid-solubility limit is approached. The same general behaviour of α with respect to electron concentration has been also observed by Smallman & Westmacott (1957), as in Fig. 1 and by Davies & Cahn (1962) and Foley, Cahn & Raynor (1963) in some copper and silver base alloys. Increase of α implies a lowering of the stacking fault energy γ and if we assume a rougly inverse relationship between the stacking fault probability α and the stacking fault energy γ (Vassamillet, 1961), then this general form of the curves is in approximate agreement with the electron microscope observations (Howie & Swann, 1961) of the variation of γ as a function of electron concentration in several alloys of copper and silver. The qualitative agreement is also revealed in Fig. 2, which shows the variation of α^{-1} with solute content.

It is apparent from Fig. 1 that for fixed e/a, fault probability α increases in the order Cu–In, Cu–Sn which is consistent with the fact that, for fixed electron/atom ratio, α increases as the solute valency increases (Davies & Cahn, 1962; Adler & Wagner, 1962; Sen Gupta & Quader, 1966). The values of α for copper–tin alloys, as reported by Smallman & Westmacott (1957), are found to be less than the present values. This difference in faulting frequency may be partially due to three factors, *viz.* differences in filing temperatures (Vassamillet & Massalski, 1963), the amount of cold-work put in and maintained, and the method of obtaining peak positions.

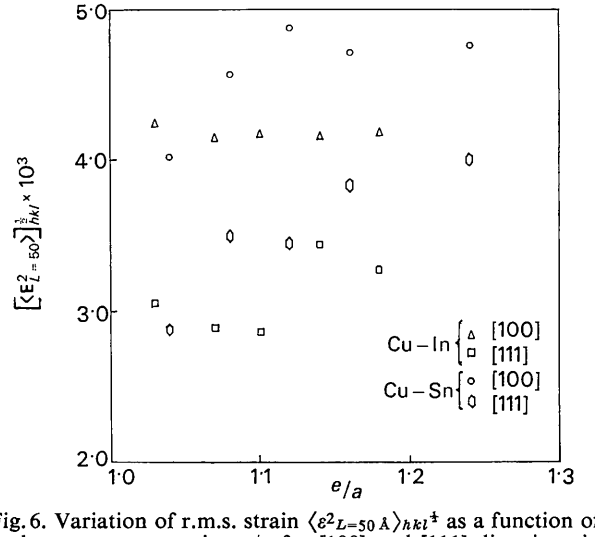

Fig. 6. Variation of r.m.s. strain $\langle\varepsilon^2_{L=50\,\text{Å}}\rangle^{\frac{1}{2}}_{hkl}$ as a function of electron concentration e/a for [100] and [111] directions in cold-worked copper-indium and copper-tin alloys.

Corresponding to the increase in α with solute concentration, the twin fault probability β also rises as the solute concentration is increased (Tables 1 and 2). However, it was not possible to obtain consistent values for β as the method suffers from experimental limitations.

The anisotropy of effective particle sizes and lattice strains has been clearly observed (Tables 1 and 2 and Figs. 3, 4 and 5). The effective particle size D_{eff}, measured by Fourier analysis of peaks, may be written in terms of the coherently diffracting domain size D normal to the reflecting planes, the deformation and twin fault probabilities α and β, the domain size T in the faulting planes and the lattice parameter a (Warren, 1961):

$$\frac{1}{[D_{\text{eff}}]_{111}} = \frac{1}{D} + \frac{1}{\sqrt{2}T} + \frac{\sqrt{3}}{4a}(1{\cdot}5\alpha+\beta)\,. \qquad (5)$$

$$\frac{1}{[D_{\text{eff}}]_{100}} = \frac{1}{D} + \frac{1}{\sqrt{1{\cdot}5}T} + \frac{1}{a}(1{\cdot}5\alpha+\beta)\,. \qquad (6)$$

The inverse of the last term is referred to as D_{SF}, the fictitious domain size due to faulting. Warren (1961) has also shown that a minimum value of T is given by:

$$T_{\min} = \frac{0{\cdot}82}{\left[\dfrac{2{\cdot}31}{[D_{\text{eff}}]_{111}} - \dfrac{1}{[D_{\text{eff}}]_{100}}\right]}\,. \qquad (7)$$

It is observed from Figs. 2 and 5 that both the effective particle size D_e and the reciprocal stacking fault probability α^{-1} and β^{-1} decrease with the increase of solute concentration in a similar way and, further, for a given amount of solute present, D_e values in the copper–tin alloys are smaller than in the copper–indium alloys of corresponding concentration in either direction. This indicates, considering the above relations, that the contribution of the stacking faults in the observed particle size broadening is significant. This is further supported by the fact that measured values of $[D_e]_{111}/[D_e]_{100}$ are very close to the theoretically predicted values of 2·3 for $[D_e]_{111}/[D_e]_{100}$ and the computed values of $[D_{SF}]_{111}$ agree fairly well with $[D_e]_{111}$ obtained from line broadening. $[D_{SF}]_{111}$ is slightly larger, as it should be when the contribution of the two terms associated with D and T to the effective particle size is taken into consideration. The average experimental ratio of $[D_e]_{111}/[D_e]_{100}$ is 1·8 and 1·9 for copper–indium and copper–tin alloys respectively and this indicates that D and more likely T (as $T_{\min}$ is slightly larger than $[D_e]_{111}$) also influence the magnitudes of the measured effective particle sizes. Values of $T_{\min}$ suggest that, in the drastic cold work which results from filing, the stacking faults tend to extend over distances which are com-

parable to the coherent domain dimensions D. A significant contribution of stacking faults to the particle size broadening has been also observed in α-CuZn (Warren & Warekois, 1955; Wagner, 1957*a*).

Measured anisotropic particle sizes also yield some information about the compound fault probability $(1{\cdot}5\alpha+\beta)$ and it has been observed (Tables 1 and 2) that values of $(1{\cdot}5\alpha+\beta)$ obtained from anisotropic particle size measurements are in fair agreement with the values obtained from peak position and peak asymmetry measurements in both cases.

The r.m.s. strains seem to vary rapidly with distance in the material for small L values, whereas for increasing L this change is small (Fig. 4). The same form of the curve was exhibited by all the specimens in both directions and has been also observed in the α-CuZn alloys (Warren & Warekois, 1955). The decrease with increasing L might be due to the fact that the strains are highly inhomogeneous. The trend of the curve at higher L is consistent with the dislocation arrangement in the materials. Owing to long range interactions of stresses around a dislocation, the positive and negative stresses balance at some average distance away from the source of stress reaching an asymptotic value. Tables 1 and 2 show the values of r.m.s. strains at an average distance $L=50$ Å and a gradual increase is observed with solute concentrations. The strain values are anisotropic and the ratio of r.m.s. strains measured at $L=50$ Å and also averaged over the distance L from 40 to 100 Å is about 1·3. However, this observed anisotropy of strain cannot be accounted for by the simple isotropic stress model according to which the residual microstrains in the [*hkl*] direction will be inversely proportional to the directional Young's modulus. From the elastic constants of copper (Huntington, 1958) (as no information is available on the elastic constants of copper–indium and copper–tin alloys) it can be shown that $E_{[111]}/E_{[100]}=2{\cdot}9$. Thus, it appears that the observed anisotropy of strain is probably related to the non-uniform distribution of dislocations and to the stress directionality (Cottrell, 1953) of dislocations and stacking faults. The strain values are higher in copper–tin alloys (Fig. 6) and this additional amount of strain is due to the higher density of dislocations resulting from the increased concentration of stacking faults (Fig. 1) in this system.

The authors are grateful to Prof. B. N. Srivastava, D.Sc., F.N.I., for his keen interest in the work. One of the authors (S.P.S.G.) is thankful to the Council for Scientific and Industrial Research (New Delhi) for financial assistance.

References

ADLER, R. P. I. & WAGNER, C. N. J. (1962). *J. Appl. Phys.* **33**, 3451.
BARRETT, C. S. (1950). *Trans. Amer. Inst. Mining, Met. Petrol Engrs.* **188**, 123.
COHEN, J. B. & WAGNER, C. N. J. (1962). *J. Appl. Phys.* **33**, 2073.
COTTRELL, A. H. (1953). *Dislocations and Plastic Flow in Crystals*, p. 73. Oxford: Clarendon Press.
DAVIES, R. G. & CAHN, R. W. (1962). *Acta Metallurg.* **10**, 621.
FOLEY, J. H., CAHN, R. W. & RAYNOR, G. V. (1963). *Acta Metallurg.* **11**, 355.
GREENOUGH, G. B. (1952). *Progr. Metal Phys.* **3**, 176.
HOWIE, A. & SWANN, P. R. (1961). *Phil. Mag.* **6**, 1215.
HUNTINGTON, H. B. (1958). *Solid State Phys.* **7**, 213.
LADELL, J., PARRISH, W. & TAYLOR, J. (1959). *Acta Cryst.* **12**, 253.
PATERSON, M. S. (1952). *J. Appl. Phys.* **23**, 805.
PAPOULIS, A. (1955). *Rev. Sci. Instrum.* **26**, 423.
RACHINGER, W. A. (1948). *J. Sci. Instrum.* **25**, 254.
SEN GUPTA, S. P. & QUADER, M. A. (1966). *Acta Cryst.* **20**, 798.
SMALLMAN, R. E. & WESTMACOTT, K. H. (1957). *Phil. Mag.* **2**, 669.
STOKES, A. R. (1948). *Proc. Phys. Soc.* B **61**, 382.
VASSAMILLET, L. F. & MASSALSKI, T. B. (1964). *J. Appl. Phys.* **35**, 2629.
VASSAMILLET, L. F. & MASSALSKI, T. B. (1963). *J. Appl. Phys.* **34**, 3398.
VASSAMILLET, L. F. (1961). *J. Appl. Phys.* **32**, 778.
WAGNER, C. N. J. (1957*a*). *Acta Metallurg.* **5**, 527.
WAGNER, C. N. J. (1957*b*). *Acta Metallurg.* **5**, 477.
WARREN, B. E. (1959). *Progr. Metal Phys.* **8**, 147.
WARREN, B. E. (1961). *J. Appl. Phys.* **32**, 2428.
WARREN, B. E. & WAREKOIS, E. P. (1955). *Acta Metallurg.* **3**, 473.